



ACADEMIC  
PRESS

Available online at [www.sciencedirect.com](http://www.sciencedirect.com)

SCIENCE @ DIRECT®

Journal of Solid State Chemistry 172 (2003) 412–416

JOURNAL OF  
SOLID STATE  
CHEMISTRY

<http://elsevier.com/locate/jssc>

# A new lead Mo(IV) phosphate with a tunnel structure: $\text{Pb}_2\text{Mo}_2\text{O}(\text{PO}_4)_2\text{P}_2\text{O}_7$

A. Leclaire,\* J. Chardon, and B. Raveau

Laboratoire CRISMAT, ISMRA UMR, 6508 CNRS, 6 bd Maréchal Juin, 14050 Caen cedex, France

Received 4 August 2002; received in revised form 12 November 2002; accepted 26 November 2002

## Abstract

A molybdenum (IV) phosphate containing lead,  $\text{Pb}_2\text{Mo}_2\text{O}(\text{PO}_4)_2\text{P}_2\text{O}_7$ , has been synthesized for the first time. It crystallizes in the space group  $C2/c$  with  $a = 14.098(1)$  Å,  $b = 14.187(2)$  Å,  $c = 6.5592(4)$  Å and  $\beta = 102.08(1)^\circ$ . Its original tunnel structure, built up of  $\text{Mo}_2\text{O}_{11}$  bioctahedra,  $\text{P}_2\text{O}_7$  and  $\text{PO}_4$  phosphate groups can be described from the assemblage of  $[\text{Mo}_4\text{P}_4\text{O}_{24}]_\infty$  ribbons interconnected through monophosphate groups. The stereoactivity of the  $6s^2$  lone pair of  $\text{Pb}^{2+}$ , which is surrounded by nine oxygen atoms, is discussed.

© 2003 Elsevier Science (USA). All rights reserved.

## 1. Introduction

Previous studies carried out on molybdenum phosphates have shown the possibility to generate numerous frameworks containing Mo(V) species. In contrast, the number of Mo(IV) phosphates actually known is rather small. Besides the molybdenum pyrophosphate  $\text{Mo}_2\text{P}_2\text{O}_7$  [1–2], four Mo(IV) phosphates containing univalent cations— $\text{NaMo}_2(\text{PO}_4)_3$  [3] and  $\text{AMo}_2\text{O}(\text{PO}_4)_2\text{P}_2\text{O}_7$  with  $A = \text{K}, \text{Rb}, \text{Tl}$  [4,5]—and only one Mo(IV) phosphate of divalent cation,  $\text{BaMo}(\text{PO}_4)_2$  [6], have been isolated.

Among those Mo(IV) phosphates, the compounds  $\text{AMo}_2\text{O}(\text{PO}_4)_2\text{P}_2\text{O}_7$  exhibit a rather unusual structural behavior, since their tunnel structure is built up of bioctahedral units “ $\text{Mo}_2\text{O}_{11}$ ”, in contrast to the other ones characterized by isolated  $\text{MoO}_6$  octahedra. Moreover, the framework of the latter phosphates contains two sorts of tetrahedral units—single  $\text{PO}_4$  tetrahedra and diphosphate groups  $\text{P}_2\text{O}_7$ —whereas only one kind of tetrahedral units is observed in other Mo(IV) phosphates. In order to better understand the crystal chemistry of Mo(IV) phosphates, the system  $\text{Pb}-\text{Mo}^{\text{IV}}-\text{P}-\text{O}$  was explored. We report herein on the synthesis and crystal structure of the first lead Mo(IV) phosphate,  $\text{Pb}_2\text{Mo}_2\text{O}(\text{PO}_4)_2\text{P}_2\text{O}_7$ , which exhibits like the  $\text{AMo}_2\text{O}$

$(\text{PO}_4)_2\text{P}_2\text{O}_7$  series, bioctahedral  $\text{Mo}_2\text{O}_{11}$  units and two kinds of tetrahedral units,  $\text{PO}_4$  and  $\text{P}_2\text{O}_7$  groups.

## 2. Synthesis and crystal growth

### 2.1. Exploration of the $\text{Pb}-\text{Mo}^{\text{IV}}-\text{P}-\text{O}$ system and synthesis of $\text{Pb}_2\text{Mo}_2\text{O}(\text{PO}_4)_2\text{P}_2\text{O}_7$

The exploration of the system was carried out in two steps, aiming at the discovery of a new phase. First, mixtures of  $\text{PbCO}_3$ ,  $\text{H}(\text{NH}_4)_2\text{PO}_4$  and  $\text{MoO}_3$  were heated in a platinum crucible and then, in a second step, metallic molybdenum powder was added and heated at high temperatures in sealed tube in order to realize different formulations. By this method, a new phase could be synthesized starting for the first step with the mixture  $\text{PbCO}_3/\text{H}(\text{NH}_4)_2\text{PO}_4/\text{MoO}_3$  in the ratio 3:6:2 heated at 673 K, and then adding in the second step 1 mol Mo and heating the intimate mixture at 1073 K for 12 h. The color of the so-obtained powder is variable, ranging from metallic green to dark gray with dark green glance.

### 2.2. Crystal growth

Single crystals were grown from a mixture of nominal composition “ $\text{PbP}_2\text{Mo}_2\text{O}_{10}$ ”. Similar to the previous synthesis,  $\text{PbCO}_3$ ,  $\text{H}(\text{NH}_4)_2\text{PO}_4$  and  $\text{MoO}_3$  were mixed

\*Corresponding author. Fax: +33-2-3195-1600.

E-mail address: [andre.leclaire@ismra.fr](mailto:andre.leclaire@ismra.fr) (A. Leclaire).

in an agate mortar, but with different ratios, i.e. 3:6:4, and heated at the same temperature (673 K) in air in order to decompose the phosphate and the carbonate. In the second step, the resulting mixture was crushed and added with 2 mol metallic Mo powder and with 5 wt% weight  $\text{PbCl}_2$  in order to lower the fusion temperature. The intimate mixture was heated for 12 h at 873 K in an evacuated silica ampoule and cooled down at  $3.5 \text{ K h}^{-1}$  down to 473 K and finally quenched to room temperature. Dark green crystals with a metallic glance were extracted from a black sintered product.

Note that for crystal growth as well as for synthesis, the cationic composition was systematically checked by

energy dispersive spectroscopy (EDS) using a Link Isis analyzer mounted on a Philips XL 30 FE 6 scanning electron microscope. In this way, the cationic composition of the single crystals and that of the pure powder samples were established to be “ $\text{Pb}_2\text{Mo}_2\text{P}_4$ ”.

The X-ray powder diffraction pattern of the powder sample can be easily indexed with the cell parameters obtained from the single-crystal X-ray study.

### 3. Crystal structure determination

A dark green crystal with dimensions  $0.045 \times 0.050 \times 0.054 \text{ mm}^3$  was selected for the structure determination after tests made with film techniques on a Weissenberg camera.

The cell parameters (Table 1) were determined with a least-squares method using 25 reflections with  $18^\circ < \theta < 22^\circ$ . The data were recorded at room temperature on an Enraf-Nonius CAD4 diffractometer using  $\text{MoK}\alpha$  radiation ( $\lambda = 0.71073 \text{ \AA}$ ) isolated with a graphite monochromator. Intensities were checked by monitoring three standard reflections every hour. No significant deviation in intensities was observed. The intensity data were corrected for Lorentz, polarization and absorption effect. The absorption corrections were computed by the Gaussian method, taking into consideration the shape of the crystal. The reflections show the monoclinic symmetry and the systematic extinctions  $h + k = 2n + 1$  for all the reflections,  $l = 2n + 1$  for  $h0l$  and  $k = 2n + 1$  for  $0k0$  are characteristic of the space group  $C2/c$ . The structure was solved with the heavy-atom method. The full-matrix least-squares refinements were performed on the  $F$  weighted by  $1/\sigma(F^2)$  with the Xtal 3.7 package [7]; the latter leads to  $R = 0.0282$  and  $R_w = 0.0248$  and to the atomic parameters of Table 2.

Table 1

Summary of crystal data, intensity measurement and structure refinement for  $\text{Pb}_2\text{Mo}_2\text{O}(\text{PO}_4)_2(\text{P}_2\text{O}_7)$

Chemical formula	$\text{Pb}_2\text{Mo}_2\text{O}(\text{PO}_4)_2(\text{P}_2\text{O}_7)$
Molecular weight	986.165 D
Crystal system	Monoclinic
Space group	$C2/c$ (15)
Cell dimensions	$a = 14.098(1) \text{ \AA}$ $b = 14.187(2) \text{ \AA}$ $c = 6.5592(4) \text{ \AA}$ $\beta = 102.080(6)^\circ$
Cell volume	$1282.8(2) \text{ \AA}^3$
$Z$	4
Density	$5.106 \text{ g cm}^{-3}$
$\mu$	$28.675 \text{ mm}^{-1}$
$T_{\text{min}}$	0.2951
$T_{\text{max}}$	0.4176
Extinction (Zacchariasen)	0.063(5)
Measured reflections	5251
Reflections with $I > 3\sigma(I)$	2032
$R_{\text{inter}}$	0.0297
Temperature of the data collections	$21^\circ\text{C}$
Number of variables	111
$R(F_o)$	0.0282
$R_w$	0.0248

Table 2

Atomic coordinates of  $\text{Pb}_2\text{Mo}_2\text{O}(\text{PO}_4)_2(\text{P}_2\text{O}_7)$

	$x$	$y$	$z$	$U_{\text{eq}}^a$	$U_{11}$	$U_{22}$	$U_{33}$	$U_{12}$	$U_{13}$	$U_{23}$
Pb(1)	0.37351(2)	0.11621(2)	0.04190(4)	0.0124(1)	0.01007(9)	0.0130(1)	0.0141(1)	0.0004(1)	0.00213(7)	0.0011(1)
Mo(1)	0.13299(4)	0.14231(4)	0.31353(8)	0.0073(2)	0.0059(2)	0.0067(2)	0.0090(2)	-0.0004(2)	0.0009(2)	-0.0003(2)
P(1)	0.3878(1)	0.4032(1)	0.1972(2)	0.0079(7)	0.0080(6)	0.0082(7)	0.0078(6)	-0.0005(5)	0.0022(5)	-0.0004(5)
P(2)	0.1272(1)	0.3660(1)	0.4630(3)	0.0090(7)	0.0073(6)	0.0091(7)	0.0102(6)	-0.0002(6)	0.0010(5)	-0.0003(6)
O(1)	0	0.1316(4)	1/4	0.014(3)	0.007(2)	0.010(3)	0.025(3)	0	0.001(2)	0
O(2)	0.1217(3)	0.2851(3)	0.3032(7)	0.011(2)	0.013(2)	0.006(2)	0.013(2)	0.001(2)	0.000(2)	-0.002(2)
O(3)	0.2808(3)	0.1472(3)	0.3663(6)	0.012(2)	0.010(2)	0.014(2)	0.011(2)	0.000(2)	-0.000(2)	0.004(2)
O(4)	0.1400(4)	0.1509(3)	0.6274(7)	0.017(3)	0.031(3)	0.007(2)	0.015(2)	-0.005(2)	0.011(2)	0.001(2)
O(5)	0.1565(4)	-0.0003(3)	0.3307(8)	0.018(2)	0.017(2)	0.007(2)	0.029(3)	-0.005(2)	0.001(2)	-0.002(2)
O(6)	0.1380(4)	0.1554(3)	0.0006(7)	0.016(2)	0.028(3)	0.012(2)	0.008(2)	-0.001(2)	0.000(2)	-0.003(2)
O(7)	1/2	0.4205(6)	1/4	0.029(4)	0.009(3)	0.036(5)	0.041(5)	0	0.003(3)	0
O(8)	0.0445(3)	0.3652(3)	0.5819(7)	0.016(2)	0.010(2)	0.022(3)	0.018(2)	-0.000(2)	0.006(2)	-0.003(2)
O(9)	0.1281(4)	0.4559(3)	0.3367(7)	0.017(3)	0.025(3)	0.010(2)	0.015(2)	0.000(2)	0.002(2)	0.002(2)

<sup>a</sup>  $U_{\text{eq}} = (\sum U_{ii})/3$ .

#### 4. Results and discussion

The projection of the structure of this phosphate along  $\vec{c}$  (Fig. 1) shows that its original framework  $[\text{Mo}_2\text{P}_4\text{O}_{16}]_\infty$  is built up, like that of  $\text{AMo}_2\text{O}(\text{PO}_4)_2\text{P}_2\text{O}_7$  [4,5], of bioctahedral “ $\text{Mo}_2\text{O}_{11}$ ” groups, diphosphate  $\text{P}_2\text{O}_7$  and monophosphate  $\text{PO}_4$  groups. Like for the latter phosphates, one observes that one  $\text{P}_2\text{O}_7$  group and one  $\text{Mo}_2\text{O}_{11}$  unit share two apices belonging to two different octahedra and two different tetrahedra. Nevertheless, the topology of the framework is very different in the two compounds. In the present framework, the entire structure can be described by the assemblage of  $[\text{Mo}_4\text{P}_4\text{O}_{24}]_\infty$  ribbons running along  $\vec{c}$  (see the brick-like arrangement in Fig. 1) interconnected through single  $\text{PO}_4$  tetrahedra. The nature of the  $[\text{Mo}_4\text{P}_4\text{O}_{24}]_\infty$  ribbons is better seen from the projection of the structure along  $\vec{b}$  (Fig. 2). Each  $[\text{Mo}_4\text{P}_4\text{O}_{24}]_\infty$  ribbon is built up from two  $[\text{Mo}_2\text{P}_2\text{O}_{14}]_\infty$  chains (Fig. 3a) where one bioctahedral unit  $\text{Mo}_2\text{O}_{11}$  alternates with one  $\text{P}_2\text{O}_7$  group along  $\vec{c}$ . In these ribbons, each  $\text{Mo}_2\text{O}_{11}$  unit of one  $[\text{Mo}_2\text{P}_2\text{O}_{14}]_\infty$  chain shares two apices with each  $\text{P}_2\text{O}_7$  group of the other chain (Fig. 3b). Note also that the  $[\text{Mo}_2\text{P}_2\text{O}_{14}]_\infty$  chains can also be described as the assemblage of  $[\text{MoPO}_8]_\infty$  chains (Fig. 3a) classically observed in many molybdenum phosphates.

The mixed framework delimits tunnels running along  $\vec{c}$  (Fig. 1) which are bordered by the monophosphate groups. The latter have two free corners pointing towards the tunnel axis, forming a bottleneck, so that

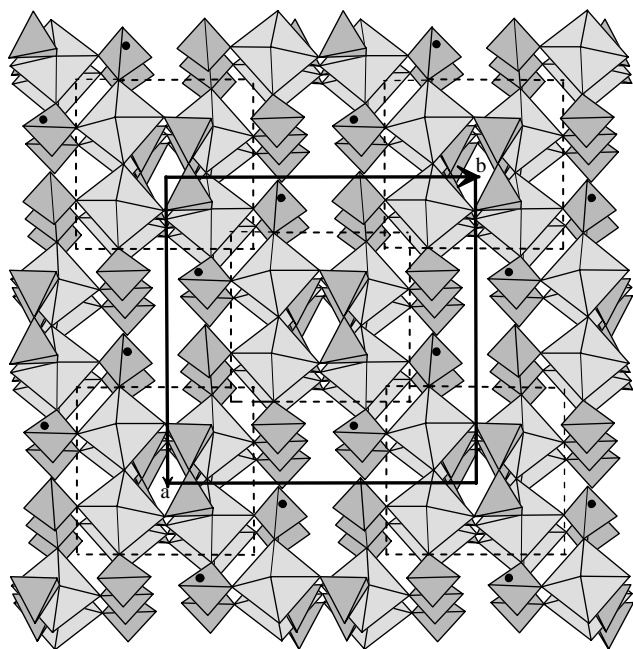


Fig. 1. Projection of the structure of  $\text{Pb}_2\text{Mo}_2\text{O}(\text{PO}_4)_2\text{P}_2\text{O}_7$  along  $\vec{c}$  (a little tilted to avoid Escher-like picture) showing the  $[\text{Mo}_4\text{P}_4\text{O}_{24}]_\infty$  ribbons running along  $\vec{c}$  (brick-like arrangement underlined by dotted lines).

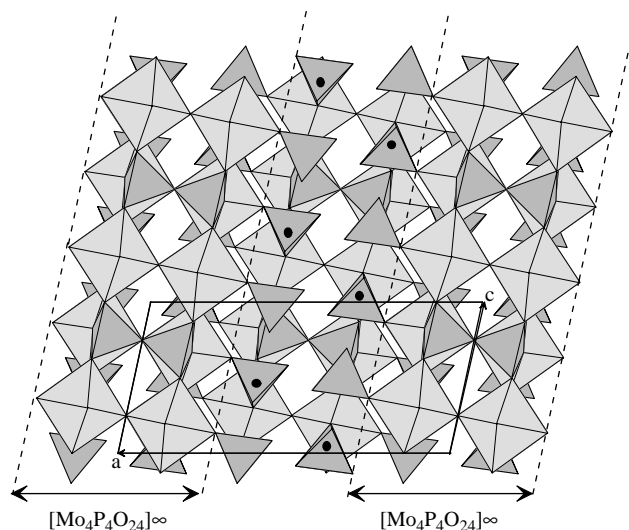


Fig. 2. Projection of the structure of  $\text{Pb}_2\text{Mo}_2\text{O}(\text{PO}_4)_2\text{P}_2\text{O}_7$  along  $\vec{b}$  showing the  $[\text{Mo}_4\text{P}_4\text{O}_{24}]_\infty$  ribbons running along  $\vec{c}$ .

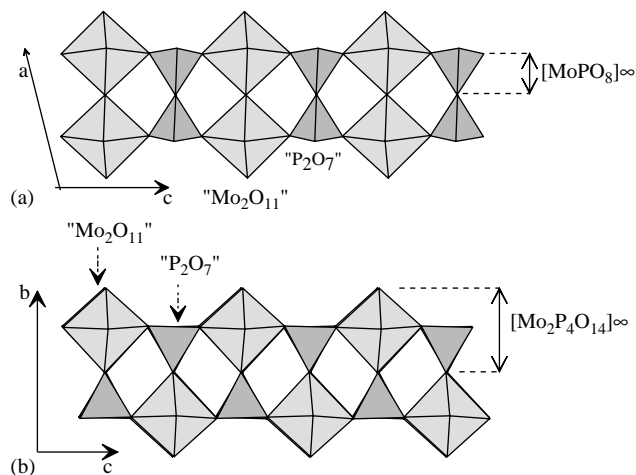


Fig. 3. (a) The  $[\text{Mo}_2\text{P}_2\text{O}_{14}]_\infty$  chains built of corner-sharing  $\text{Mo}_2\text{O}_{11}$  and  $\text{P}_2\text{O}_7$  units. (b)  $[\text{Mo}_4\text{P}_4\text{O}_{24}]_\infty$  ribbons running along  $\vec{c}$  (view along  $\vec{a}$ ) built up of  $[\text{Mo}_2\text{P}_2\text{O}_{14}]_\infty$  chains.

the tunnels are better described as successive cages stacked along  $\vec{c}$ .

The geometry of the  $\text{Mo}^{\text{IV}}\text{O}_6$  octahedra, with one short Mo–O bond [1.840(1) Å], corresponding to the oxygen atom bridging the two molybdenum atoms of the  $\text{Mo}_2\text{O}_{11}$  unit (Table 3) and five medium bonds [2.032(4)–2.077(4) Å], is similar to those previously observed in the phosphates  $\text{AMo}_2\text{O}(\text{PO}_4)_2\text{P}_2\text{O}_7$  [4,5]. As usually observed, the geometry of the  $\text{PO}_4$  tetrahedron belonging to a diphosphate group shows a longer bond [1.566(2) Å] corresponding to the oxygen atom bridging two phosphorous atoms, and three shorter ones [1.500(5)–1.520(5) Å]. The monophosphate group exhibits two long P–O distances corresponding to the oxygen atoms shared with the molybdenum and two shorter ones corresponding to the “free corners”.

Table 3  
Interatomic distances (Å) and angles (°) in  $\text{Pb}_2\text{Mo}_2\text{O}(\text{PO}_4)_2(\text{P}_2\text{O}_7)$

Mo(1)	O(1)	O(2)	O(3)	O(4)	O(5)	O(6)
O(1)	<b>1.840(1)</b>	2.749(7)	3.879(6)	2.838(4)	2.856(6)	2.813(5)
O(2)	90.3(2)	<b>2.032(4)</b>	2.941(6)	2.826(6)	4.077(6)	2.751(7)
O(3)	175.7(2)	92.4(2)	<b>2.041(4)</b>	2.881(7)	2.708(6)	2.793(6)
O(4)	93.8(2)	87.8(2)	89.7(2)	<b>2.044(5)</b>	2.938(7)	4.106(7)
O(5)	94.4(2)	175.3(2)	82.9(2)	91.7(2)	<b>2.049(5)</b>	3.066(7)
O(6)	91.6(2)	84.1(2)	85.4(2)	170.3(2)	96.0(2)	<b>2.077(5)</b>
P(1)	O(4 <sup>i</sup> )	O(5 <sup>ii</sup> )	O(6 <sup>iii</sup> )	O(7)		
O(4 <sup>i</sup> )	<b>1.502(5)</b>	2.504(7)	2.455(7)	2.497(6)		
O(5 <sup>ii</sup> )	113.0(3)	<b>1.500(5)</b>	2.505(7)	2.434(6)		
O(6 <sup>iii</sup> )	108.6(3)	112.1(3)	<b>1.520(5)</b>	2.512(6)		
O(7)	108.9(3)	105.0(3)	109.0(3)	<b>1.566(2)</b>		
P(2)	O(2)	O(3 <sup>i</sup> )	O(8)	O(9)		
O(2)	<b>1.545(4)</b>	2.503(6)	2.578(7)	2.433(6)		
O(3 <sup>i</sup> )	108.6(3)	<b>1.537(4)</b>	2.421(6)	2.556(6)		
O(8)	113.8(3)	104.1(3)	<b>1.533(5)</b>	2.535(7)		
O(9)	105.0(3)	113.4(3)	112.2(3)	<b>1.523(5)</b>		

Symmetry codes: i:  $\frac{1}{2} - x, \frac{1}{2} - y, 1 - z$ ; ii:  $\frac{1}{2} - x, \frac{1}{2} + y, \frac{1}{2} - z$ ; iii:  $\frac{1}{2} - x, \frac{1}{2} - y, -z$ .

The Mo–O or P–O distances are on the diagonal and the O...O distances above it and the O–Mo–O or O–P–O angles under it.

Table 4  
Lead coordination in  $\text{Pb}_2\text{Mo}_2\text{O}(\text{PO}_4)_2(\text{P}_2\text{O}_7)$

Pb(1)–O(8 <sup>iv</sup> )	2.384(4) Å
Pb(1)–O(9 <sup>v</sup> )	2.412(5) Å
Pb(1)–O(8 <sup>i</sup> )	2.510(4) Å
Pb(1)–O(2 <sup>iii</sup> )	2.675(5) Å
Pb(1)–O(9 <sup>iii</sup> )	2.681(5) Å
Pb(1)–O(3)	2.755(5) Å
Pb(1)–O(6 <sup>iii</sup> )	3.253(5) Å
Pb(1)–O(6)	3.321(5) Å
Pb(1)–O(5 <sup>vi</sup> )	3.494(5) Å

Symmetry codes: i:  $\frac{1}{2} - x, \frac{1}{2} - y, 1 - z$ ; ii:  $\frac{1}{2} - x, \frac{1}{2} + y, \frac{1}{2} - z$ ; iii:  $\frac{1}{2} - x, \frac{1}{2} - y, -z$ ; iv:  $\frac{1}{2} + x, \frac{1}{2} - y, z - \frac{1}{2}$ ; v:  $\frac{1}{2} - x, y - \frac{1}{2}, \frac{1}{2} - z$ ; vi:  $x, -y, z - \frac{1}{2}$ .

The lead cation sits in the cages formed by the [001] tunnels. It is surrounded by nine oxygen atoms but three of them are sitting further apart, i.e. at distances larger than 3.2 Å (Table 4). Thus, the coordination polyhedra of  $\text{Pb}^{2+}$  can be better characterized by three shorter Pb–O bonds (2.384–2.518 Å) and three longer ones (2.675–2.755 Å). In this respect, it is similar to that observed in  $\text{Pb}_{0.9}\text{PMo}_5\text{O}_{17}$  [8]. Like in the latter compound, the six nearest oxygen atoms are indeed sitting on the same side of  $\text{Pb}^{2+}$  (Fig. 4), leaving more space for its  $6s^2$  lone pair which may be oriented in the opposite direction towards the O(5<sup>vi</sup>) and O(6) atoms. Thus, this stereoactivity of the  $6s^2$  lone pair of  $\text{Pb}^{2+}$  distorts its coordination polyhedron as in  $\text{Pb}_{0.9}\text{PMo}_5\text{O}_{17}$  [8] and in  $\text{Pb}_3(\text{MoO})_3(\text{PO}_4)_5$  [9].

Finally, the calculation of the sum of the electrostatic valences received by molybdenum and by lead, using the general Rij values of Zocchi [10], confirms the

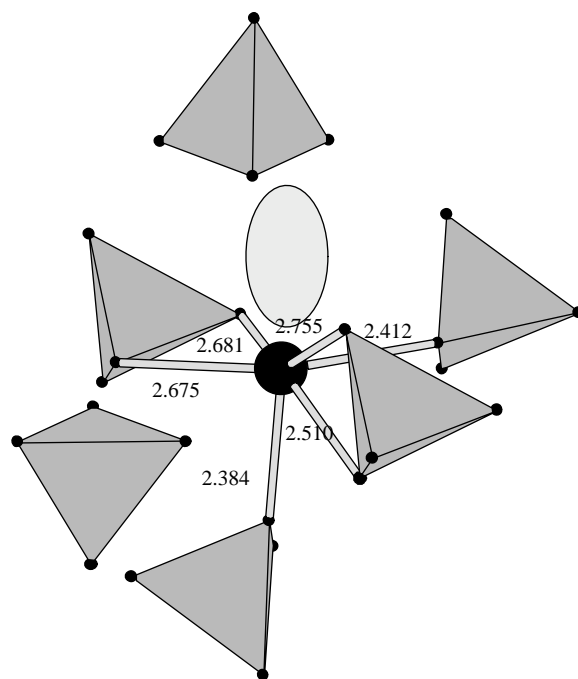


Fig. 4. The surrounding of the lead atom showing the stereoactivity of the lone pair.

tetravalency of molybdenum and the divalent character of lead (Table 5).

In conclusion, a tetravalent molybdenum phosphate containing lead has been synthesized for the first time. Its original tunnel structure contains, like  $\text{AMo}_2\text{OPO}_4$   $\text{P}_2\text{O}_7$  phosphates [4,5], bioctahedral units,  $\text{P}_2\text{O}_7$  groups

Table 5  
Electrostatic valences in  $\text{Pb}_2\text{Mo}_2\text{O}(\text{PO}_4)_2(\text{P}_2\text{O}_7)$

	Mo(1)	P(1)	P(2)	Pb(1)	$\sum e^-$
O(1)	1.136/1.136				2.272
O(2)	0.605		1.193	0.219	2.017
O(3)	0.587		1.219	0.176	1.982
O(4)	0.581	1.340			1.921
O(5)	0.572	1.348		0.024	1.944
O(6)	0.522	1.277		0.046	1.883
				0.038	
O(7)		1.127/1.127			2.254
O(8)			1.233	0.479	2.053
				0.341	
O(9)			1.266	0.445	1.926
				0.215	
$\sum e^+$	4.003	5.092	4.911	1.982	

and  $\text{PO}_4$  groups, but is fundamentally different from the latter showing the effect of the  $6s^2$  lone pair of  $\text{Pb}^{2+}$ . These results also demonstrate that in these phosphates  $\text{Pb}^{2+}$  remains stable in the presence of reduced species

$\text{Mo}^{4+}$ ; they open the route to the investigation of numerous oxides involving the  $\text{Pb}^{2+}/\text{Mo}^{4+}$  couple.

## References

- [1] L. Lezama, J.M. Rojo, J.L. Mesa, T. Rojo, R. Olazcuaga, *J. Solid State Chem.* 119 (1995) 146.
- [2] A. Leclaire, M.M. Borel, A. Grandin, B. Raveau, *Eur. J. Solid State Inorg. Chem.* 25 (1988) 323.
- [3] K.H. Lii, J.J. Chen, S.L. Wang, *J. Solid State Chem.* 78 (1989) 93.
- [4] A. Leclaire, J.C. Monier, B. Raveau, *J. Solid State Chem.* 59 (1985) 301.
- [5] A. Leclaire, B. Raveau, *Acta Crystallogr. C* 44 (1988) 226.
- [6] A. Leclaire, M.M. Borel, J. Chardon, B. Raveau, *J. Solid State Chem.* 116 (1995) 364.
- [7] S.R. Hall, D.J. du Boulay, R. Olthof-Hazekamp (Eds.), *Xtal 3.7 System*, University of Western-Australia, Australia, 2000.
- [8] A. Leclaire, J. Chardon, S. Boudin, J. Provost, B. Raveau, *Chem. Mater.* 14 (2002) 3427.
- [9] A. Leclaire, J. Chardon, J. Provost, B. Raveau, *J. Solid State Chem.* 163 (2002) 308.
- [10] F. Zocchi, *Solid State Sci.* 3 (2001) 383.